THE JOURNAL OF BIOLOGICAL CHEMISTRY
Vol. 269, No. 38, Issue of September 23, pp. 23413–23419, 1994
Printed in U.S.A.

The Solution Structure of Sarafotoxin-c

IMPLICATIONS FOR LIGAND RECOGNITION BY ENDOTHELIN RECEPTORS*

(Received for publication, March 24, 1994)

Robyn G. Mills, Greg B. Ralston, and Glenn F. King‡

From the Department of Biochemistry, University of Sydney, Sydney, New South Wales 2006, Australia

The solution structure of sarafotoxin-c has been determined using NMR spectroscopy. A total of 112 interproton distance constraints derived from two-dimensional NMR spectra were used to calculate a family of structures using a combination of distance geometry and dynamical simulated annealing calculations. The structures reveal a well defined α-helix extending from Glu^9 to Cys^{15} and an N-terminal region (Cys^1–Asp^8) that is tightly constrained by disulfide bonds to Cys residues in the central helix. In contrast, the C-terminal region (His^{16}–Trp^{21}) does not adopt a defined conformation in the final family of structures. This is consistent with the paucity of NMR-derived structural constraints obtained for this region and leads to the suggestion that the C-terminal region oscillates rapidly between a number of substantially different conformers. It is proposed that differences between the central helix of the endothelin and sarafotoxin isopeptides might be important in binding of these ligands by the G protein-coupled endothelin receptors.

The sarafotoxins (SRTXs)[1] are highly toxic vasopressor peptides synthesized in the venom gland of the snake genus *Atractaspis* (Kochva *et al.*, 1993). They have powerful cardiac effects in mammals, with intravenous administration of 5 μg of venom to mice typically causing cardiac arrest and death within several minutes (Kochva *et al.*, 1982). The four isoforms that have been isolated from snake venom, SRTX-a, -b, -c, and -d, exhibit strong sequence similarity (57–62%) with the endothelin (ET) isopeptides, ET-1, -2, and -3, which has led to their grouping into a single ET/SRTX superfamily (Landan *et al.*, 1991). All members of the ET/SRTX family contain 21 residues with strictly conserved disulfide bridges between Cys^1 and Cys^{15}, and Cys^3 and Cys^{11}.

The ETs were discovered in 1988 and are now known to to be the most active pressor molecules in the mammalian vasculature (Yanagisawa *et al.*, 1988). They primarily act as paracrine hormones involved in blood pressure homeostasis, and their biological actions are mediated by several G protein-coupled receptors that bind specific isoforms with high affinity (Simonson, 1993). There are three receptor subtypes that are pharmacologically distinct and that have been cloned: the ET_A receptor has greater affinity for ET-1 and ET-2 over ET-3 (Arai *et al.*, 1990), the ET_C receptor has greater affinity for ET-3 over ET-1 and ET-2 (Karne *et al.*, 1993), and the ET_B receptor binds all three isoforms with equal avidity (Sakurai *et al.*, 1990).

The ET/SRTX superfamily of peptides has stimulated enormous interest in the past few years due to the postulated role of ET in the etiology of a number of cardiovascular diseases such as hypertension, myocardial ischemia, and congestive heart failure. There are numerous reports of raised plasma ET levels in these pathophysiological states (*e.g.* Miyauchi *et al.* (1991)) as well as evidence of altered expression of ET receptors (*e.g.* Gulati and Rebello (1991)). While the role of ET in hypertension remains controversial, it was recently reported (Yokokawa *et al.*, 1991) that two patients with a rare ET-secreting malignant hemiangioendothelioma of the scalp had high blood pressure, which was ameliorated by removal of the tumors, thus directly implicating ET in the etiology of this disease.

Consequently, much research has been devoted to understanding structure-function relationships within the ET/SRTX peptides in order to facilitate the rational design of receptor antagonists that might aid the clinical management of cardiovascular disorders in which ET is thought to be involved. Initial structure-function studies targeted the roles of conserved residues in ET-1-mediated vasoconstriction. The two disulfide bonds, particularly Cys^1–Cys^{15}, the free amino group presented by the N terminus, and the hydrophobic C-terminal region, especially the terminal Trp^{21} residue, have all been claimed to contribute to ET-1-induced vasoconstriction (*e.g.* Kimura *et al.* (1988), Hirata *et al.* (1989), Randall *et al.* (1989), and Topouzis *et al.* (1989, 1991)). It was also postulated that variations in net charge in the intramolecular loop resulting from the Cys^3–Cys^{11} disulfide bond contributed to differences in receptor affinity and specificity (Sokolovsky, 1992). Therefore, the emerging picture was that structural elements contributing to peptide function are distributed throughout the full length of the molecule and that few residues can be discounted in the search for determinants of receptor binding and biological activity.

Numerous NMR studies have attempted to discern the solution conformation of the ET/SRTX peptides. Interpretation and comparison of these structures is extremely difficult and must be done with extreme caution as they have been obtained using a wide range of solvents, with very few studies reporting the structure of the peptides in biologically relevant aqueous solutions. While all studies agree on a helical conformation between residues 9 and 15, a consensus has not yet been reached for the C-terminal conformation (*e.g.* Endo *et al.* (1989), Saudek *et al.* (1991), Bortmann *et al.* (1991), Mills *et al.* (1991, 1992), and Andersen *et al.*, 1992)).

In this paper, we report the structure of SRTX-c in aqueous solution. The sequence of this isoform differs from all other ET/SRTX peptides at position 9 where it has a Glu rather than a Lys residue. SRTX-c has been singled out as an ET_B-specific ligand (Williams *et al.*, 1991), consistent with the observation

* This work was supported by a research grant (to G. F. K.) and a postgraduate science research scholarship (to R. G. M.) from the Australian National Heart Foundation. The costs of publication of this article were defrayed in part by the payment of page charges. This article must therefore be hereby marked "*advertisement*" in accordance with 18 U.S.C. Section 1734 solely to indicate this fact.

‡ To whom correspondence should be addressed. Tel.: 61-2-692-3902; Fax: 61-2-692-4726; E-mail: gfking@extro.ucc.su.oz.au.

[1] The abbreviations used are: SRTX, sarafotoxin; DQF-COSY, double quantum-filtered *J*-correlated spectroscopy; ET, endothelin; NOE, nuclear Overhauser enhancement; NOESY, NOE spectroscopy; r.m.s., root mean square; d_4-TSP, 3-trimethylsilyl[2,2,3,3-^{2}H]propionate; τ_m, NOESY mixing period.

that a $Lys^9 \rightarrow Glu$ substitution increases the ET_B binding affinity and decreases the ET_A binding affinity of other ET_B agonists (Takai *et al.*, 1992). We present evidence that SRTX-c contains a well defined central α-helix, similar to that previously reported for SRTX-b (Mills *et al.*, 1991) but different from the generally irregular helix reported for ET peptides (*e.g.* Bortmann *et al.* (1991) and Mills *et al.* (1992)). It is proposed that differences between the central helix of the ET and SRTX isopeptides might be important in the binding of these ligands by ET receptors. We also analyze the role of the conformationally flexible C-terminal region in receptor binding and discuss why the constrained C-terminal analogue, BQ123, is a potent antagonist of the ET_A receptor.

EXPERIMENTAL PROCEDURES

Materials—SRTX-c (amino acid sequence CTCNDMTDEECLNFCHQDVIW) was purchased from American Peptide Co. (Santa Clara, CA). 3-Trimethylsilyl[2,2,3,3-^{2}H]propionate (d_4-TSP) was from Fluka A.G. (Buchs, Switzerland). Dr. Peter Güntert kindly provided the distance geometry program DIANA (Güntert *et al.*, 1991), while the molecular dynamics program X-PLOR was from Prof. Axel Brünger (Brünger, 1990). Molecular superpositions were performed using the SUPPOS program (Gröningen BIOMOL protein structure package), which uses the method of Kabsch (1976) to calculate the rotation for optimal superposition of a pair of structures. All spectral analysis and molecular superpositions were performed on a Sun SPARCstation 2GX computer. Structure calculations were performed using a Silicon Graphics Indigo R4000 workstation. Molecular graphics were displayed on a Silicon Graphics Indigo 4D/20G workstation using the programs MidasPlus (Computer Graphics Laboratory, University of California) (Ferrin *et al.*, 1988), Insight II (Biosym Inc., San Diego, CA), and MOLSCRIPT (Kraulis, 1991).

Analytical Ultracentrifugation Experiments—Sedimentation equilibrium measurements were made at 30,000 and 40,000 rpm in a Beckman Optima XL-A analytical ultracentrifuge with the use of 6-channel equilibrium centerpieces (Yphantis, 1964). Sample loadings of 120 µl were used, giving a solution depth of 2 mm at concentrations of 0.5, 1.0, and 2.0 g liter^{-1}. Scans taken at 5 and 9 h were found to be identical within the precision of the measurements.

The composition of the peptide was used to calculate a value of 0.691 ml g^{-1} for the partial specific volume in water (Cohn and Edsall, 1943) and a value of 2.4 liters g^{-1} cm^{-1} for A_{280} (Gill and von Hippel, 1989). The density of water at 30 °C was taken to be 0.996 g ml^{-1}, and that of 100 mM NaCl at 30 °C was taken to be 1.000 g ml^{-1}.

Scans were taken at 280 nm with the lowest loading concentration, for which the absorbance ranged between 0.8 and 1.7 at equilibrium, and at 300 nm with the two higher loadings, for which the absorbance ranged between 0.3 and 1.4. Scans taken after attainment of sedimentation equilibrium were corrected for background absorbance, arising from partial masking of light pulses or from window imperfections, by subtraction of a scan taken at 360 nm. The concentration distribution at equilibrium was analyzed by means of Beckman software running under Origin™.

NMR Experiments—SRTX-c was dissolved at a final concentration of 2.5 mM in a 100 mM NaCl solution prepared using 95% H_2O, 5% D_2O solvent (pH 3.77). The solution also contained sodium azide (1 mM) as a bactericide and d_4-TSP (0.1 mM) as a chemical shift reference.

All NMR experiments were performed at 37 °C using a Bruker AMX-600 narrow bore spectrometer equipped with a dedicated proton probe. All experiments were collected using standard pulse sequences, except for double quantum-filtered *J*-correlated spectroscopy (DQF-COSY) spectra, which were collected using the modified phase cycling of Derome and Williamson (1990). The raw data for each two-dimensional experiment consisted of 432–560 t_1 increments, with each free induction decay consisting of 64–128 scans. Prior to Fourier transformation, spectra were processed using a combination of Lorentz-Gauss and shifted sine-bell functions or, alternatively, using a skewed sine-bell function that was shifted by 60 and 90 ° in the F_2 and F_1 dimensions, respectively. Following zero filling in both dimensions, the final transformed data matrices were typically 4096 × 1024 ($F_2 \times F_1$) real data points. Base lines were corrected using a third-order polynomial function that was fitted to and then subtracted from the rows and columns of the transformed matrices. Chemical shifts were referenced to the methyl resonance of d_4-TSP at 0.00 ppm.

A spectral width of 6.8 kHz was employed in all experiments, and continuous coherent saturation of the water resonance was performed during the relaxation time in all two-dimensional experiments as well as during the mixing period of two-dimensional NOESY experiments. The spin lock in two-dimensional total correlation spectroscopy experiments, which was obtained using an MLEV-17 isotropic mixing sequence (Bax and Davis, 1985), had a radiofrequency field strength of ~10 kHz.

The buildup of NOESY cross-peak intensity was followed by acquiring NOESY spectra with mixing times (τ_m) ranging from 150 to 450 ms. Those cross-peaks that only appeared at the largest mixing times were assessed to result from spin diffusion and were not included in interproton distance calibrations. Proton-proton distance constraints were derived from cross-peak intensities in a NOESY spectrum collected with τ_m = 350 ms; this NOESY spectrum represented a suitable compromise between reasonable cross-peak intensity and minimal spin diffusion effects.

Structure Calculations—Cross-peaks observed in NOESY spectra were converted to the following upper distance bounds according to their intensity as judged by contour levels: 2.8 Å (strong), 3.3 Å (medium), and 4.5 Å (weak). Lower distance bounds in all calculations were taken to be the sum of the van der Waals radii. The disulfide bridges, Cys^1–Cys^{15} and Cys^3–Cys^{11}, were fixed in all structure calculations by constraining the S–S distance to an upper limit of 2.1 Å and S–βC distances across each bridge to an upper limit of 3.1 Å (Williamson *et al.*, 1985). Pseudoatoms with appropriate distance corrections were employed for protons that could not be stereospecifically assigned (Wüthrich *et al.*, 1983).

The 169 ^{1}H–^{1}H distance constraints obtained from NOESY cross-peak intensities were filtered through the distance geometry program, DIANA, to eliminate irrelevant constraints (*i.e.* those distances that are predetermined by the covalent geometry of the molecule or for which no possible conformation will violate the constraints). The remaining 112 constraints (22 intraresidue, 54 sequential, and 36 medium to long range constraints) were used in subsequent structure calculations.

DIANA was used to calculate 1000 structures from random starting conformations. The 61 best structures (selected on the basis of their final penalty function values) were then refined in X-PLOR using dynamical simulated annealing (Nilges *et al.*, 1988). We employed the six-stage protocol described previously (Mills *et al.*, 1992) with the following modifications: k_{bond} was set to 1000 kcal mol^{-1} Å^{-2} (rather than 500 kcal mol^{-1} Å^{-2}) during the two rounds of energy minimisation, interatomic distances were constrained using k_{NOE} = 10 kcal mol^{-1} Å^{-2}, and, in stage 2, the dynamic trajectory was followed for 20 ps rather than 10 ps.

RESULTS

Ultracentrifugation Experiments—Self-association can be problematic in NMR studies of proteins if the exact oligomeric state of the protein is unknown. Symmetric dimers are particularly difficult to work with as it is impossible *a priori* to distinguish between intra- and intermonomer dipolar connectivities in NOESY spectra (*e.g.* O'Donoghue *et al.* (1993)). While analytical ultracentrifugation experiments showed that ET-1 is largely monodisperse at concentrations up to ~3.0 g liter^{-1} in 10% acetic acid (Tamaoki *et al.*, 1991), it has been claimed that surface tension measurements indicate the protein aggregates to form micelles at concentrations above 0.2 g liter^{-1} in pure water (Bennes *et al.*, 1990). Thus, it was imperative to establish whether SRTX-c self associates under the conditions of the NMR experiments.

Sedimentation equilibrium experiments showed that SRTX-c was monomeric in both water and 100 mM NaCl up to a concentration of 3 g liter^{-1} and showed no tendency up to this concentration to self associate. The distribution at equilibrium accounted for all of the material placed in the cell. The concentration distribution at sedimentation equilibrium for the individual channels could be fitted adequately with a model for a single nonassociating species, with best estimate molecular weights between 2100 and 2700, as shown in Fig. 1 for 2.0 g liter^{-1} SRTX-c in water. The distribution of residuals was visually random. For both solvents, no improvement in fit was obtained by including a second virial coefficient, and the best estimate of the second virial coefficient was not significantly

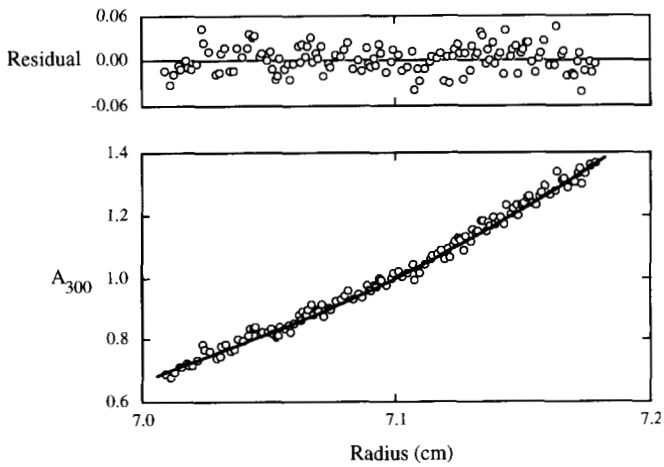

FIG. 1. **Sedimentation equilibrium analysis of SRTX-c.** The data points show the measured concentration distribution (as a function of radial distance) of SRTX-c in water at sedimentation equilibrium. The initial loading concentration was 2.0 g liter^{-1}. The *solid line* shows the best fit with a model of a single, ideal, nonassociating solute component with a molecular weight of 2590, in good agreement with the value of 2512 calculated from the sequence.

different from zero. Global fitting of all three channels in a single experiment with a single molecular weight yielded a best estimate molecular weight of 2290 in 100 mM NaCl and 2610 in water, in good agreement with the value determined from the sequence of 2512.

Spectral Assignment and Analysis—Analysis of SRTX-c spectra was made difficult by the unusually large number of αCH resonances that were near to, or obscured by, the solvent resonance. This problem was also experienced in our previous studies of SRTX-b (Mills *et al.*, 1991) and ET-3 (Mills *et al.*, 1992), where it was alleviated by shifting the water resonance downfield by decreasing the pH and/or temperature. In the case of SRTX-c, αCH resonances overlapping with the H_2O resonance were assigned by acquiring DQF-COSY spectra in D_2O. To exemplify the difficulty of assigning αCH resonances in the two-dimensional NMR spectra of these peptides, the αCH-βCH region of the DQF-COSY spectrum of SRTX-c in D_2O is displayed in Fig. 2. The majority of αCH resonances have chemical shifts near ~4.7 ppm, which is coincident with the resonance of H_2O under the pH and temperature conditions used.

Analysis of DQF-COSY and total correlation spectroscopy spectra enabled sequence-specific assignment of resonances from the unique residues Met[6], Leu[12], Val[19], and Ile[20]. It was also possible to make residue-specific assignment of resonances arising from the Thr, Glu, and Gln residues. Sequence-specific assignment of these resonances, as well as those arising from the 12 AMX-type spin systems, required analysis of dipolar connectivities in NOESY spectra. A summary of the NOE connectivities observed in the spectra of SRTX-c is presented in Fig. 3. Sequential βCH-NH connectivities (all residue pairs except 5–6, 7–8, and 14–15) and sequential NH-NH connectivities between residues 3–6, 7–8, and 9–19 enabled unique spin system assignment. As only 10 out of a possible 20 sequential αCH-NH connectivities were visible in the two-dimensional NOESY spectra of SRTX-c, these assignments lent support to the proposed assignments rather than directing the assignment process. Complete chemical shift assignments for SRTX-c are given in Table I.

Examination of the observed NOEs (Fig. 3) reveals not only a stretch of sequential NH-NH connectivities between residues 9 and 19 but also a large number of medium range connectivities (*i.e.* $d_{i,i+3}$, $d_{i,i+4}$) in the region 9–15, all of which are indicative of helical secondary structure (Wüthrich, 1986). Few interactions are observed in the C-terminal region of SRTX-c, and no long range NOEs are evident between the putative helix and the C-terminal residues. Hence, qualitative evaluation of the observed NOEs indicates a helical conformation in the region 9–15, with no evidence of association between this helix and residues in the C-terminal region.

Calculation of Tertiary Structure—Following distance geometry/dynamical simulated annealing calculations, four structures with violations of the NMR-derived distance restraints greater than 0.5 Å were excluded from analysis. The remaining 57 structures displayed good covalent geometry (mean r.m.s. differences from ideal bond lengths and bond angles were 0.0045 ± 0.0004 Å and 0.50 ± 0.05°, respectively) and good nonbonded contacts, as evidenced by the negative mean Lennard-Jones potential of −144 ± 14 kcal mol^{-1}. Furthermore, the structures displayed no violations of bonds >0.05 Å nor of angles or improper angles >5°. A summary of structural statistics for the family of structures is presented in Table II.

Various views of the final family of 57 SRTX-c structures are shown in Fig. 4. The backbone conformation of residues 1–15 is tightly constrained (Fig. 4*A*), and residues Glu[9]–Cys[15] form a right-handed α-helix (Figs. 4, *A* and *B*). In contrast, the C-terminal segment (His[16]–Trp[21]) adopts a relatively undefined conformation with no consistent orientation with respect to the central helix. The convergence of the family of structures in Cartesian space, as assessed by comparing the mean r.m.s. differences of the family from the structure with the least violations of the experimental distance restraints, gives a good indication of which regions of the molecule are structurally well defined and which regions are conformationally flexible. For segments 1–15, 9–15, and 16–21, the mean r.m.s. differences for backbone atoms (C, αC, and N) are 1.08 ± 0.35, 0.35 ± 0.12, and 1.64 ± 0.44 Å; this compares with a mean r.m.s. difference of 3.39 ± 0.68 Å calculated for the backbone atoms of the entire molecule. Fig. 5 demonstrates the good superposition of the ϕ and ψ dihedral angles in the region 9–21. The average ϕ and ψ values over the region 9–15 of −68° and −32°, respectively, are consistent with recently reported values for a typical α-helix (ϕ = −63°, ψ = −42°) (Benedetti *et al.*, 1992). The quality of superposition in Cartesian and torsion angle space is consistent with the number and distribution of constraints (Clore and Gronenborn, 1991). The family of 57 structures, as well as an energy-minimized average structure, will be deposited in the Brookhaven Protein Data Bank.

DISCUSSION

All NMR studies of the ET/SRTX peptides have yielded a helical conformation for residues 9–15, although its pitch and/or regularity varies considerably between studies. While it would be useful to attempt to decipher differences in receptor-subtype binding by the various ET/SRTX isoforms in terms of these putative conformational differences, this task is made extremely difficult because of the range of solvents used in the various NMR studies. The conformations of at least certain members of this peptide superfamily appear to be solvent-dependent; for example, the central helix of ET-1 has been variously described as irregular in 100% dimethyl sulfoxide (Endo *et al.*, 1989), pseudo α-helical in 40–75% ethylene glycol (Andersen *et al.*, 1992), and α-helical in 10% acetic acid (Tamaoki *et al.*, 1991). Thus, as in our previous studies of SRTX-b (Mills *et al.*, 1991) and ET-3 (Mills *et al.*, 1992), we chose to study the structure of SRTX-c in a physiologically relevant aqueous solution (100 mM NaCl in H_2O); under these conditions, SRTX-c has no tendency to self associate and the region Glu[9]–Cys[15] forms a regular α-helix.

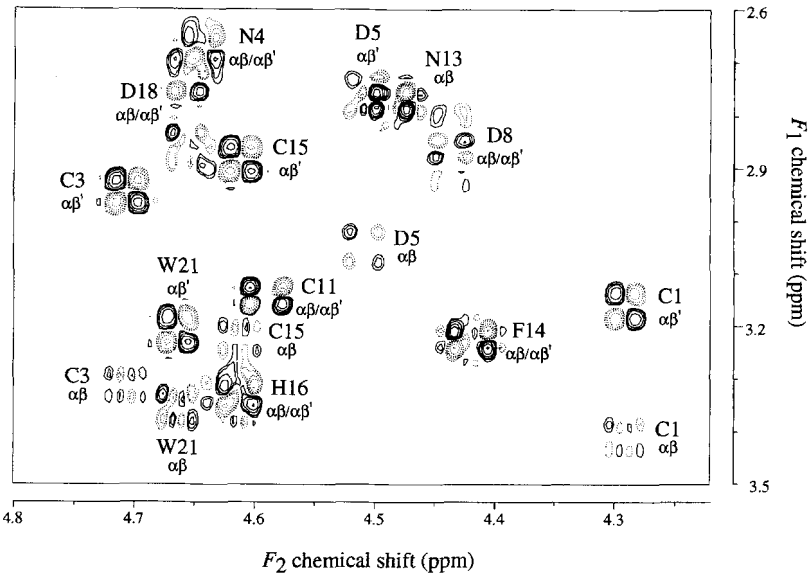

FIG. 2. **αCH-βCH region of a DQF-COSY spectrum of SRTX-c.** *Continuous* and *dotted lines* indicate positive and negative contours, respectively. Assignments are given adjacent to each cross-peak. Note that the majority of αCH-βCH cross-peaks occur in a small region centered around an F_2 chemical shift of 4.7 ppm, which is almost coincident with the large water resonance in spectra obtained in H_2O. Chemical shifts differ slightly from the values quoted in Table I because of a small difference in pH; this is especially true of the Asp residues, which have pK_a values near the pH used in NMR experiments.

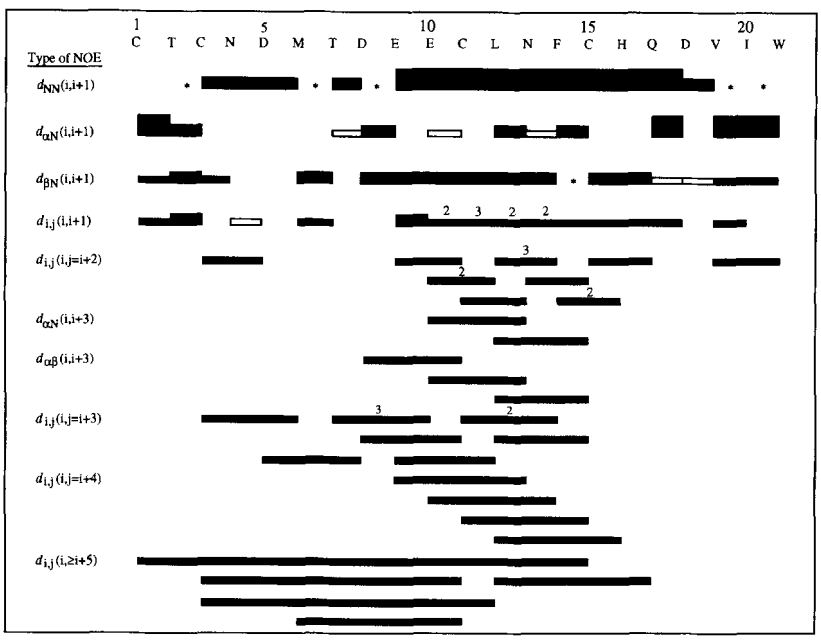

FIG. 3. **Summary of NOESY connectivities observed for SRTX-c.** The *solid bars* indicate the presence of an NOE, and the height of the bar is proportional to the NOE intensity. *Open bars* indicate NOEs that were not deemed structurally relevant by the program DIANA (see text) and were, therefore, not used in structure calculations. *Asterisks* indicate NOEs that could not be unequivocally assigned due to chemical shift degeneracy. Where any particular type of NOE occurs more than once, the number of occurrences is given *above* the *bar*. An NOE between sidechain protons on residues i and j is represented by d_{ij}.

Tamaoki *et al.* (1992) carried out an extensive CD study of the ET/SRTX peptides dissolved in H_2O and H_2O/trifluoroethanol mixtures. CD spectra of SRTX-b and -c dissolved in H_2O displayed classic α-helical characteristics (positive ellipticity at 192 nm, a negative minimum at 208 nm, and a shoulder at 223 nm). CD spectra of ET-1 and -2 dissolved in H_2O showed little evidence of α-helicity, but this could be induced by the addition of trifluoroethanol. ET-3, on the other hand, did not appear to contain any regular α-helix even in the presence of trifluoroethanol. The authors consequently proposed that there is an intrinsic difference in the helical characteristics of the SRTX and ET families. The tertiary structures we have determined for SRTX-b, SRTX-c, and ET-3, all in aqueous solution, lend credence to this conclusion. The stylized representations of these structures in Fig. 6 clearly indicate that the central helices of SRTX-b and -c are largely α-helical, while that of ET-3 is very much irregular as noted previously (Mills *et al.*, 1992).

Thus, it is tempting to classify these peptides according to their extents of α-helix formation. However, transient formation of α-helical secondary structure is often obscured in CD spectra by motional averaging (*e.g.* Dyson *et al.* (1988)). It may be inappropriate to limit descriptions of small flexible peptides, albeit in this case stabilized by disulfide bridges, to the pitch and length of the given motif. Rather than attempting to establish whether the peptide assumes a discrete α-helical configuration (or not), it is considered preferable to consider what percentage of conformer populations might occupy this region of (ϕ, ψ) space and to compare how the ensemble of conformers varies between ET/SRTX peptides. The consistent observation of an α-helix in calculated SRTX structures may be the result of this being the predominant (but not the only) conformer, while the variable results obtained for ET peptides may reflect a different ensemble of conformers (presumed to include α-helical conformations), which is sensitive to the solvent environment. The irregular helix consistently observed in NMR-de-

TABLE I
Proton resonance assignments for SRTX-c at pH 3.77 and 310 K

Residue	Chemical shift[a]			
	NH	αCH	βCH	Others
			ppm	
Cys[1]	4.30	3.40	3.17	
Thr[2]	8.77	4.58	4.12	γCH 1.20
Cys[3]	8.68	4.72	2.93, 3.30	
Asn[4]	8.31	4.65	2.67	
Asp[5]	8.57	4.53	2.72, 3.02	
Met[6]	7.96	4.68	1.80, 2.18	γCH_2 2.40, 2.55; ϵCH_3 1.75
Thr[7]	8.07	4.44	4.62	γCH 1.28
Asp[8]	8.52	4.46	2.83, 2.90	
Glu[9]	8.54	4.01	2.03, 2.09	γCH_2 2.47
Glu[10]	7.80	4.11	2.10, 2.20	γCH_2 2.51
Cys[11]	8.36	4.60	3.15	
Leu[12]	8.06	3.99	1.56, 1.76	γCH 1.68; δCH_3 0.84
Asn[13]	7.66	4.49	2.76	γNH_2 6.86, 7.44
Phe[14]	8.26	4.43	3.22	δCH 7.32; εCH 7.40; ζCH 7.36
Cys[15]	8.44	4.60	2.89, 3.23	
His[16]	7.96	4.62	3.33	ϵ_1CH 8.55; δ_2CH 7.23
Gln[17]	8.15	4.33	1.96, 2.10	γCH_2 2.33
Asp[18]	8.32	4.67	2.73, 2.87	
Val[19]	7.81	4.02	1.86	γCH_3 0.64, 0.76
Ile[20]	7.88	4.13	1.76	γCH_2 1.07, 1.35; γCH_3 0.84; δCH_3 0.80
Trp[21]	7.80	4.67	3.34, 3.18	δ_1CH 7.21; ϵ_3CH 7.66; ζ_3CH 7.13; η_2CH 7.20; ζ_2CH 7.46; ϵ_1NH 9.33

[a] Chemical shifts are referenced internally to the methyl resonance of d_4-TSP at 0.00 ppm.

TABLE II
Summary of structural statistics for the family of SRTX-c structures

Structural statistic	Value for SRTX-c
Number of constraints	112
Number of final refined structures	57
Average violation of NOE constraints	0.043 ± 0.009 Å
Violations of NOE constraints >0.5 Å	None
Dihedrals in allowed Ramachandran regions[a]	96%
Mean r.m.s. differences from ideal geometry	
Bonds	0.0045 ± 0.0004 Å
Angles	0.50 ± 0.05°
Impropers	0.43 ± 0.08°
Violations of bonds >0.05 Å	None
Violations of angles or impropers >5°	None
Mean final energies (kcal mol^{-1})	
Total	−107 ± 25
Bonds	7 ± 1
Angles	22 ± 5
Impropers	5 ± 2
Lennard-Jones	−11 ± 10
Coulombic	−145 ± 14
NOE	15 ± 6
Atomic r.m.s. differences	
Residues 1–21	3.4 ± 0.7 Å
Residues 1–15	1.08 ± 0.35 Å
Residues 3–11	0.74 ± 0.27 Å
Residues 9–15	0.35 ± 0.12 Å
Residues 16–21	1.6 ± 0.4 Å

[a] The overall percentage of (ϕ,ψ) dihedral angles, which are found in allowed regions of the Ramachandran plot according to the program Procheck (Morris *et al.*, 1992). Of the final family of 57 structures, 20 had no Ramachandran violations, 35 had one violation (always Asp^8), and two had two violations (Asp^8 and Cys^3).

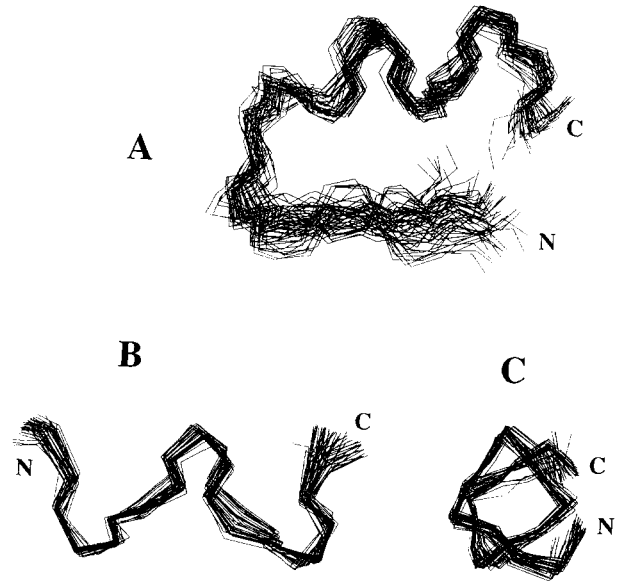

FIG. 4. **Family of structures calculated for SRTX-c in aqueous solution.** The backbones (N, αC, and C atoms) of all 57 structures are shown for residues 1–15 (*A*) and for the central helix (residues 9–15) viewed both side-on (*B*) and looking down the helix axis (*C*). The structures are superimposed on the best structure for minimum r.m.s. difference over either residues 1–15 (*A*), or residues 9–15 (*B* and *C*). The *N*- and *C*-terminal ends are labeled in each view. The C-terminal region (residues 16–21) is poorly constrained in three-dimensional space (backbone r.m.s. difference of 1.64 ± 0.44 Å) and is consequently not shown for the sake of clarity.

rived ET-3 structures (Bortmann *et al.*, 1991; Mills *et al.*, 1992) might be an artifact of the calculations employed, which assume the existence of a single discrete conformation that satisfies all of the NMR-derived distance constraints. Indeed, we have recently shown (Mills, 1994) that the NMR data for ET-3 is better fitted using time-averaged constraints (Torda *et al.*, 1990) in which the structure is not modelled as a single discrete conformation but as the time-average of an ensemble of structures.

Thus, while the grouping of the ET/SRTX peptides proposed by Tamaoki *et al.* (1992) is not challenged, the rationale is modified. The accessibility of α-helical space to ET-3 is not ruled out but considered a far less favored state than for other isoforms. Due to sequence differences, ET-3 may more easily interchange between a wider ensemble of isoenergetic conformations than in the cases of ET-1 and -2. It is proposed that the presence of α-helical conformers, clearly evident in both NMR and CD studies of SRTX peptides, is obscured by different extents of conformational averaging in the various ET isoforms. The relative helicity of the ET/SRTX peptides may modulate the range of conformers present in each isoform and more importantly the percentage of time spent in the particular con-

former, which is recognized and bound by the receptor. Thus, this interpretation does not preclude ET from forming, however transiently, a largely α-helical motif, which is recognized by the receptor.

The most complete model to date of ligand recognition by the ET receptors is that of Sakamoto *et al.* (1993), which was based on ligand binding by a comprehensive array of ET_A/ET_B receptor chimeras. This model essentially proposes that the variable N-terminal region of the ET peptides, which encompasses the two disulfide bonds, acts as an "address domain," which determines the specificity of receptor binding, while the invariant C-terminal region acts as a "message domain," which is responsible for signal transduction. More specifically, Sakamoto *et al.* (1993) suggested that transmembrane regions 4–6 of the ET_A receptor recognized the N-terminal region of ET-1, due to the putative role of the free amino group at the N terminus in vasoconstriction and the absence of the N-terminal region in two ET analogues, IRL1620 (*N*-α-succinyl-[$Ala^{11,15}$]ET-1(8–21)) and BQ3020 (*N*-acetyl-[$Ala^{11,15}$]ET-1(6–21)), which act as ET_B-selective agonists. The promiscuity of the ET_B receptor was proposed to result from a relatively nonspecific address recognition site, or a "self content" address domain, which therefore made it nonobligatory for the ligand to present address information. However, given the ~2-fold greater selectivity of [$Ala^{1,3,11,15}$]ET-1 over BQ3020 for the ET_B receptor (Saeki *et al.*, 1991; Ihara *et al.*, 1992), and ~1000-fold greater selectivity of IRL1620 over IRL1038 ([Cys^{11}–Cys^{15}]ET-1(11–21)) (Urade *et al.*, 1992), the interaction of residues in the N-terminal region and the intramolecular Cys^3–Cys^{11} loop with transmembrane regions 4–6 of the ET_B receptor should not be overlooked as a determinant of ET_B affinity and selectivity.

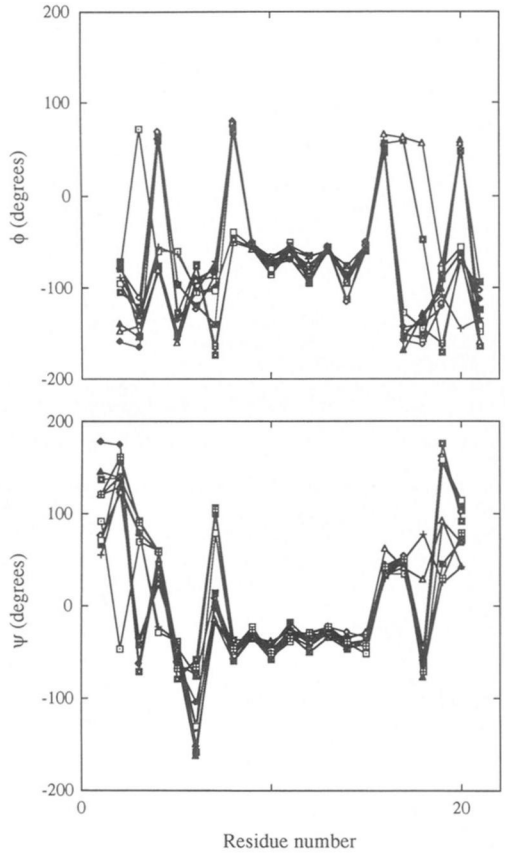

FIG. 5. **Overlay of ϕ and ψ backbone dihedral angles for the best 10 SRTX-c structures.** Good convergence is observed for both the ϕ and ψ angles in the central helix (residues 9–15), whereas dihedral angles in the N- and C-terminal regions are more divergent.

Within the Sakamoto model, it is possible to suggest a role for the central helix in the ET/SRTX peptides. This region might be likened to the "spacer" or "linker" structure found in opioid antagonists; the receptor selectivity of these bivalent ligands is considered to be related to the flexibility and distance imposed by the spacer (Takemori and Portoghese, 1992). The relative stability of the central helix in the ET/SRTX peptides and their relative propensities to "fray" at the ends (Andersen *et al.*, 1992) might regulate the relative presentation of the C-terminal message and N-terminal address domains to the receptor. Furthermore, the macrodipole associated with helical conformers might have functional implications through the modulation of pK_a values of charged residues placed at the N or C termini of the helices.

The exact role of the C-terminal region of the ET/SRTX peptides in receptor binding is difficult to define. The proposal by Sakamoto *et al.* (1993) that this region acts as the message domain for the ET receptors and is thus responsible for signal transduction is largely based on conservation of its primary structure (His-Gln/Leu-Asp-Val/Ile-Ile-Trp) in the various members of this superfamily of peptides. However, this suggestion seems discrepant with the observation that BQ123, a cyclic pentapeptide (cyclo-(D-Asp-L-Pro-D-Val-L-Leu-D-Trp)), which mimics the C terminus of the ET/SRTX peptides, is an antagonist rather than an agonist of the ET_A receptor. Furthermore, despite the high primary structure homology in the C-terminal region of the ET/SRTX peptides, various NMR studies have indicated vastly different conformations for this region of the peptides, ranging from well defined for ET-3 (*e.g.* Bortmann *et al.* (1991) and Mills *et al.* (1992)) to conformationally disordered (*e.g.* SRTX-c in this study). It may be, however, that Sakamoto's proposal is correct and that conformational flexibility in the C-terminal region is necessary to enable binding to a deep-seated site in the ET receptor in a manner that promotes signal transduction (Williams, 1977); indeed, studies of G protein-coupled receptors that recognize other ligands indicate that the membrane-spanning regions of the receptor form a deep hydrophobic cleft into which the ligands must penetrate and move along to reach the receptor-activation site (Hibert *et al.*, 1993;

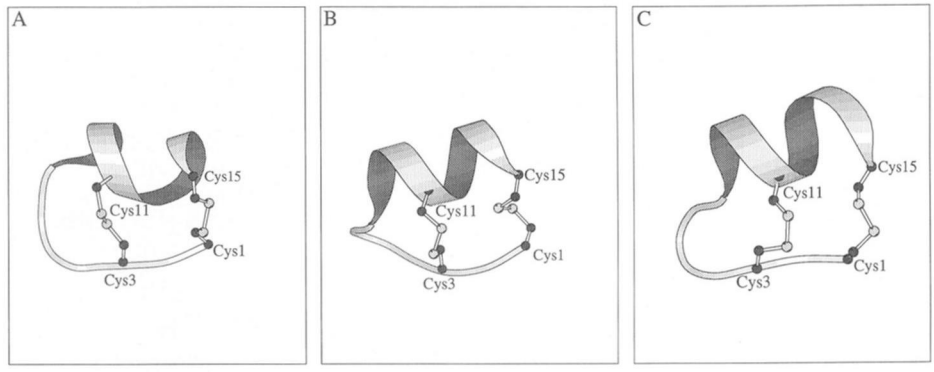

FIG. 6. **Schematic representations of the solution structures of ET-3 (*A*) (Mills *et al.*, 1992), SRTX-b (*B*) (Mills *et al.*, 1991), and SRTX-c (*C*) (this study).** These cartoons, which encompass only residues 1–15 of each of the peptides, were generated using the program MOLSCRIPT (Kraulis, 1991). The 4 conserved Cys residues are labeled, and the two disulfide bonds are shown in ball-and-stick representation.

Savarese and Fraser, 1993). Through the use of a fluorescent probe, the ligand-binding site of the hamster β_2-adrenergic receptor has been estimated to be 11–12 Å from the external surface of the receptor, or approximately one-third of the way down the transmembrane helical core (Tota and Strader, 1990). Hence, BQ123, despite its superficial similarity to the proposed ET/SRTX message domain, may be a receptor antagonist rather than agonist, because the structural constraints imposed by cyclization prevent the conformational adjustments in the receptor and ligand, which are prerequisites for signal transduction.

In summary, the structure of SRTX-c determined in this study, in combination with those previously determined for SRTX-b and ET-3 (Mills *et al.*, 1991, 1992), have led to the postulate that the relative stability of the central helix of these peptides might regulate the presentation of various domains to the ET receptors. Further work is clearly required to elucidate the exact nature of these domains for each of the ET receptor subtypes. However, the structural data summarized schematically in Fig. 6 is consistent with the proposal by Sakamoto *et al.* (1993) that the N-terminal region of the ET/SRTX peptides behaves as a structurally variable address domain, which determines which receptors they will bind, while the conserved C-terminal domain has inherent flexibility, which is necessary for probing a deep-seated receptor site and promoting signal transduction. We are currently investigating the dynamics of the C-terminal region of the ET/SRTX peptides in order to examine the role this might play in promoting ligand recognition and signal transduction by the ET receptors.

Acknowledgments—We thank Dr. Bill Bubb for expert help with maintenance and operation of the Bruker AMX600 NMR spectrometer, and Associate Prof. Richard Christopherson for helpful discussions.

REFERENCES

Andersen, N. H., Chen, C., Marschner, T. M., Krystek, S. R., Jr., and Bassolino, D. A. (1992) *Biochemistry* **31,** 1280–1295

Arai, H., Hori, S., Aramori, I., Ohkubo, H., and Nakanishi, S. (1990) *Nature* **348,** 730–732

Bax, A., and Davis, D. G. (1985) *J. Magn. Reson.* **65,** 355–360

Benedetti, E., Di Blasio, B., Pavone, V., Pedone, C., Toniolo, C., and Crisma, M. (1992) *Biopolymers* **32,** 453–456

Bennes, R., Calas, B., Chabrier, P.-E., Demaille, J., and Heitz, F. (1990) *FEBS Lett.* **276,** 21–24

Bortmann, P., Hoflack, J., Pelton, J. T., and Saudek, V. (1991) *Neurochem. Int.* **18,** 491–496

Brünger, A. T. (1990) *X-PLOR Version 2.1,* User Manual, Yale University, New Haven, CT

Cohn, E. J., and Edsall, J. T. (1943) *Proteins, Amino Acids, and Peptides as Ions and Dipolar Ions,* pp. 370–381, Reinhold, New York

Clore, G. M., and Gronenborn, A. M. (1991) *Science* **252,** 1390–1399

Derome, A. E., and Williamson, M. P. (1990) *J. Magn. Reson.* **88,** 177–185

Dyson, H. J., Rance, M., Houghton, R. A., Wright, P. E., and Lerner, R. A. (1988) *J. Mol. Biol.* **201,** 201–217

Endo, S., Inooka, H., Ishibashi, Y., Kitada, C., Mizuta, E., and Fujino, M. (1989) *FEBS Lett.* **257,** 149–154

Ferrin, T. E., Huang, C. C., Jarvis, L. E., and Langridge, R. (1988) *J. Mol. Graphics* **6,** 13–27

Gill, S. C., and von Hippel, P. H. (1989) *Anal. Biochem.* **182,** 319–326

Gulati, A., and Rebello, S. (1991) *Life Sci.* **48,** 1207–1215

Güntert, P., Braun, W., and Wüthrich, K. (1991) *J. Mol. Biol.* **217,** 517–530

Hibert, M. F., Trumpp-Kallmeyer, S., Hoflack, J., and Bruinvels, A. (1993) *Trends Pharmacol. Sci.* **14,** 7–12

Hirata, Y., Yoshimi, H., Emori, T., Shichiri, M., Marumo, F., Watanabe, T. X., Kumagaye, S., Nakajima, K., Kimura, T., and Sakakibara, S. (1989) *Biochem. Biophys. Res. Commun.* **160,** 228–234

Ihara, M., Saeki, T., Fukuroda, T., Kimura, S., Ozaki, S., Patel., A. C., and Yano, M. (1992) *Life Sci.* **51,** 47–52

Kabsch, W. (1976) *Acta Crystallogr.* **A 32,** 922–923

Karne, S., Jayawickreme, C. K., and Lerner, M. R. (1993) *J. Biol. Chem.* **268,** 19126–19133

Kimura, S., Kasuya, Y., Sawamura, T., Shinmi, O., Sugita, Y., Yanagisawa, M., Goto, K., and Masaki, T. (1988) *Biochem. Biophys. Res. Commun.* **156,** 1182–1186

Kochva, E., Vilgoen, C. C., and Botes, D. P. (1982) *Toxicon* **230,** 581–592

Kochva, E., Bdolah, A., and Wollberg, A. (1993) *Toxicon* **31,** 541–568

Kraulis, P. J. (1991) *J. Appl. Crystallogr.* **24,** 946–950

Landan, G., Bdolah, A., Wollberg, Z., Kochva, E., and Graur, D. (1991) *Toxicon* **29,** 237–244

Mills, R. G. (1994) *Molecular Biological Studies of the Endothelin/Sarafotoxin Vasopressor Peptides.* Ph.D. dissertation, University of Sydney

Mills, R. G., Atkins, A. R., Harvey, T., Junius, F. K., Smith, R., and King, G. F. (1991) *FEBS Lett.* **282,** 247–252

Mills, R. G., O'Donoghue, S. I., Smith, R., and King, G. F. (1992) *Biochemistry* **31,** 5640–5645

Miyauchi, T., Sugishita, Y., Yamaguchi, I., Ajisaka, R., Tomizawa, T., Onizuka, M., Matsuda, M., Kono, I., Yanagisawa, M., Goto, K., Suzuki, N., Matsumoto, H., and Masaki, T. (1991) *J. Cardiovasc. Pharmacol.* **17** Suppl. 7, 394–397

Morris, A. L., MacArthur, M. W., Hutchinson, E. G., and Thornton, J. M. (1992) *Proteins Struct. Funct. Genet.* **12,** 345–364

Nilges, M., Gronenborn, A. M., Brünger, A. T., and Clore, G. M. (1988) *Protein Eng.* **2,** 27–38

O'Donoghue, S. I., Junius, F. K., and King, G. F. (1993) *Protein Eng.* **6,** 557–564

Randall, M. D., Douglas, S. A., and Hiley, C. R. (1989) *Br. J. Pharmacol.* **98,** 685–699

Saeki, T., Ihara, M., Fukuroda, T., Yamagiwa, M., and Yano, M. (1991) *Biochem. Biophys. Res. Commun.* **179,** 286–292

Sakamoto, A., Yanagisawa, M., Sawamura, T., Enoki, T., Ohtani, T., Sakurai, T., Nakao, K., Toyo-oka, T., and Masaki, T. (1993) *J. Biol. Chem.* **268,** 8547–8553

Sakurai, T., Yanagisawa, M., Takuwai, Y., Miyazaki, H., Kimura, S., Goto, K., and Masaki, T. (1990) *Nature* **348,** 732–735

Saudek, V., Hoflack, J., and Pelton, J. T. (1991) *Int. J. Pept. Protein Res.* **37,** 174–179

Savarese, T. M., and Fraser, C. M. (1992) *Biochem. J.* **283,** 1–19

Simonson, M. S. (1993) *Physiol. Rev.* **73,** 375–411

Sokolovsky, M. (1992) *J. Neurochem.* **59,** 809–821

Takai, M., Umemura, I., Yamasaki, K., Watakabe, T., Fujitani, Y., Oda, K., Urade, Y., Inui, T., Yamamura, T., and Okada, T. (1992) *Biochem. Biophys. Res. Commun.* **184,** 953–959

Takemori, A. E., and Portoghese, P. S. (1992) *Annu. Rev. Pharmacol. Toxicol.* **32,** 239–269

Tamaoki, H., Kobayashi, Y., Nishimura, S., Ohkubo, T., Kyogoku, Y., Nakajima, K., Kumagaye, S., Kimura, T., and Hayashi, M. (1991) *Protein Eng.* **4,** 509–518

Tamaoki, H., Kyogoku, Y., Nakajima, K., Sakakibara, S., Hayashi, M., and Kobayashi, Y. (1992) *Biopolymers* **32,** 353–357

Topouzis, S., Pelton, J. T., and Miller, R. C. (1989) *Br. J. Pharmacol.* **98,** 669–677

Topouzis, S., Huggins, J. P., Pelton, J. T., and Miller, R. C. (1991) *Br. J. Pharmacol.* **102,** 545–549

Torda, A. E., Scheek, R. M., and van Gunsteren, W. F. (1990) *J. Mol. Biol.* **214,** 223–235

Tota, M. R., and Strader, C. D. (1990) *J. Biol. Chem.* **265,** 16891–16897

Urade, Y., Fujitani, Y., Oda, K., Watakabe, T., Umemura, I., Takai, M., Okada, T., Sakata, K., and Karaki, H. (1992) *FEBS Lett.* **311,** 12–16

Williams, D. L., Jr., Jones, K. L., Colton, C. D., and Nutt, R. F. (1991) *Biochem. Biophys. Res. Commun.* **180,** 475–480

Williams, R. J. P. (1977) *Angew. Chem. Int. Ed. Engl.* **16,** 766–777

Williamson, M. P., Havel, T. F., and Wüthrich, K. (1985) *J. Mol. Biol.* **182,** 295–315

Wüthrich, K. (1986) *NMR of Proteins and Nucleic Acids,* pp. 117–129, John Wiley & Sons, Inc., New York

Wüthrich, K., Billeter, M., and Braun, W. (1983) *J. Mol. Biol.* **169,** 949–961

Yanagisawa, M., Kurihara, H., Kimura, S., Tomobe, Y., Kobayashi, M., Mitsui, Y., Yazaki, Y., Goto, K., and Masaki, T. (1988) *Nature* **332,** 411–415

Yokokawa, K., Tahara, H., Kohno, M., Murakawa, K., Yasunari, K., Nakagawa, K., Hamada, T., Otani, S., Yanagisawa, M., and Takeda, T. (1991) *Ann. Int. Med.* **114,** 213–215

Yphantis, D. A. (1964) *Biochemistry* **3,** 297–317